Sigma Bond Activation by Cooperative Interaction: $B^+ + CH_4 + nH_2$

Gregory I. Gellene

Department of Chemistry and Biochemistry, Texas Tech University, Lubbock, Texas 79409-1061

Received: March 31, 2003

The reactions of $B^+ + CH_4 + nH_2$ ($n = 1, 2$) to produce B^+ sigma-bonded insertion products have been studied by high-level ab initio computational techniques. The results demonstrate that the mechanism of sigma bond activation by cooperative interaction, previously identified for the $B^+ + nH_2$ and $B^+ + nCH_4$ systems, continues to operate for the $B^+ + CH_4 + nH_2$ systems. In the mixed systems, the CH and HH sigma bonds compete for the role of the "insertion" sigma bond or the "cooperating" sigma bond and CH_4 can alternatively participate as a one or two sigma bond contributor. Although the transition state separating electrostatic complexes from covalently bound B^+ insertion products may appear to favor CH insertion ($n = 1$) or HH insertion ($n = 2$), the activation energy required to convert these products is only about 20% of the available exoergicity, so that both products would be expected in practice. Remarkably, the reaction of $B^+(H_2)_2 + CH_4$ is predicted to proceed to B^+ insertion products with an activation energy of less than 1 kcal/mol.

Introduction

The activation of sigma bonds, particularly CH sigma bonds, is an active area of experimental and theoretical research and has been referred to as one of the "Holy Grails" of modern chemical research.[1] Recent theoretical studies[2−6] have identified a new mode of sigma bond activation that depends critically on the number of sigma bonds simultaneously interacting with an atom in an s^2 electron configuration. Motivated by unexpected experimental results,[7] theoretical studies[2] of this cooperative interaction mechanism first focused on the gas phase reactions: $B^+(^1S_g) + nH_2 \rightarrow BH_2^+ + (n-1)H_2$, $n = 1-4$. The calculations clearly show that the transition state structure and associated activation energy for the formation of BH_2^+ depend dramatically on the number of H_2 molecules present up to three. For $n = 1$, the reaction proceeds stepwise where first the H_2 bond is broken as one hydrogen atom is transferred to B^+, fully forming BH^+ with an activation energy of about 56.8 kcal/mol. In the second step, the other BH bond is formed with no activation energy and an overall exoergicity of about 55.9 kcal/mol relative to $B^+ + H_2$. These results were in general agreement with previous theoretical[8] and experimental[9−11] findings, although the detailed nature of the transition state had not been identified in those studies. For $n = 2$, the reaction proceeds in a concerted, one-step process through a planar cyclic transition state via a pericyclic mechanism where simultaneously both H_2 bonds are broken and two BH bonds and a new H_2 bond are formed. This mechanistic change significantly lowers the activation energy to about 8.2 kcal/mol relative to $B^+ + 2H_2$. For $n = 3$, the transition state structure is characterized by an end-on interaction of three equivalent H_2 molecules with B^+ having an activation energy of −2.7 kcal/mol with respect to $B^+ + 3H_2$. In this mechanism, BH_2^+ is ultimately formed by the insertion of B^+ into a single H_2 molecule (the only case of the three where true insertion takes place); however, the insertion occurs late in the mechanism after more than 75% of the exoergicity has been released. Although there are no direct experimental studies of the $n = 2$ reaction, mass spectrometric investigations[7] of the $n = 3$ reaction fully support the theoretical conclusions.

Subsequent theoretical studies on the isoelectronic $Li^- + nH_2$ and $Be + nH_2$ systems[4,5] and the isovalent $Al^+ + nH_2$ system[3] sought to identify how much of the activation energy lowering in the cooperative interaction mechanism could be attributed to the node structure of the orbitals, how much to the effect of the positive charge and relative bond strengths, and how much to the special ability of boron to form three-center two-electron bonds (3c−2e). The results revealed that (1) the $n = 1$ activation energy was dominantly controlled by M−H bond energy, (2) the positive charge and HM−H bond energy play important roles in the activation energy lowering occurring for $n = 2$, and (3) 3c−2e bonding played a small role in the $n = 3$ case. Thus, the positive charge, large HM−H bond energy, and the ability to form 3c−2e bonds appeared to make B^+ uniquely well suited for the cooperative interaction mechanism. This conclusion was supported by theoretical studies[6] of $B^+ + nCH_4$ which showed that the cooperative activation mechanism operated effectively with CH bonds. In particular, the activation energy for formation of the insertion product $CH_3BH^+ + CH_4$ from $B^+ + 2CH_4$ was only about 5.0 kcal/mol.

The present work extends the theoretical studies of the cooperative interaction sigma bond activation mechanism by considering the reaction series $B^+ + CH_4 + nH_2 \rightarrow$ insertion products ($n = 1, 2$). With two types of sigma bonds present (i.e., CH and HH) these systems explore the interesting question of which bonds will play the role of the cooperator and which bonds will undergo the insertion. Beyond insight into this qualitative question, two important quantitative results emerge from this study: (1) insertion products can be formed from $B^+(H_2)_2 + CH_4$ with an activation energy less than 1.0 kcal/mol and (2) rearrangement between CH and HH insertion products (i.e., products having CBH and HBH sigma bonds) can occur generally with remarkably low activation energies of only about 15 kcal/mol.

10.1021/jp0304172 CCC: $25.00
Published on Web 10/10/2003

TABLE 1: Calculated Geometries and Relative Energies for $B^+/CH_4/H_2$ Stationary Points

property	electrostatic complex	transition state 1	$CH_3BH^+(H_2)$	transition state 2	$BH_2^+CH_4$
point group	C_1	C_s	C_1	C_s	C_{2v}
$r(H_2)$/Å	0.7429	0.9193	0.7871	1.1440	
R/Å	2.6377	1.4273	1.4593	2.1048	
r(BC)	2.0314	1.7843	1.5067	1.6088	1.7623
R(BH)			1.1750	1.1699	1.1721
$\theta(R,r(H_2)$/deg	82.5	110.4	89.4	89.6	90.0
$\theta(R,r$(BC)/deg	89.2	108.7	111.6	87.6	180.0
θ(BCH′)/deg	175.4	139.5			
θ(HBC)/deg			144.2	126.9	
relative energy					
MP2/pVDZ+	−18.57	−0.33	−94.05	−74.19	−100.57
CCSD(T)/pVDZ+	−17.37	5.62	−83.30	−62.96	−90.17
MP2/pVTZ+	−19.90	0.10	−98.71	−79.28	−105.25
CCSD(T)/pVTZ+	−18.63	4.05	−89.43	−71.35	−96.12
relative ZPE	0.59	2.16	5.26	4.87	7.93

Methods

Preliminary geometry optimization and stationary point characterization were performed using the aug-cc-pVDZ basis set[12,13] (abbreviated pVDZ+) with final geometry optimization and stationary point characterization performed using the aug-cc-pVTZ basis set[12,13] (abbreviated pVTZ+). The former is of double-ζ quality and the latter is of triple-ζ quality, and both are augmented with diffuse functions that are important for describing electrostatic interactions. Pure spherical harmonic basis functions were used throughout. With the one exception of the insertion transition state for the $B^+ + CH_4 + H_2$ reaction, which will be described in more detail later, qualitatively similar results were obtained with the two basis sets.

Stationary points on the $B^+/CH_4/H_2$ and $B^+/CH_4/2H_2$ hypersurfaces were located and characterized by MP2 perturbation theory applied to a Hartree−Fock wave function with frozen core electrons. Analytical first derivatives were used to optimize the geometry of the stationary points, and analytical second derivatives were used to characterize the stationary points as a local minimum (all real frequencies) or a first-order transition state (one imaginary frequency). For each transition state identified, the local reaction coordinate was determined by displacing the geometry slightly in the direction of the eigenvector associated with the imaginary frequency (both positive and negative) and following the gradient to a subsequent stationary point.

At each stationary point identified by the MP2 calculations, coupled cluster with single and double substitutions and a perturbative treatment of triple substitutions (CCSD(T))[14] calculations were performed. All calculations were performed using the GAUSSIAN 94 suite of programs[15] on a DEC alpha 433au workstation.

Results

To facilitate comparisons between the properties of various $B^+/CH_4/nH_2$ stationary points and between previously calculated B^+/nH_2 and B^+/CH_4 stationary points,[2,6] only a subset of MP2/pVTZ+ internal coordinates will be reported. The coordinates $r(H_2)$, r(BC), and r(BH) denote the distance between hydrogen atoms in noninserted H_2, boron and carbon, and boron and hydrogen after insertion, respectively. The coordinate R denotes the distance between boron and the center of a noninserted H_2 molecule. In the angular coordinate notation, H′ denotes the hydrogen of a CH_4 molecule located furthest from boron. In the various geometries, $r(H_2)$ and R can be compared with the MP2/pVTZ+ values[2] of 0.7374 and 2.272 Å calculated for H_2 and $B^+(H_2)$, respectively. Total energies and unscaled harmonic zero-point energies (ZPEs) are reported relative to $B^+ + CH_4 + nH_2$.

Several trends in the relative energy of the various stationary points calculated at different levels of theory can be identified before discussing the individual systems in detail. In general, binding energies increase when the basis set is increased from pVDZ+ to pVTZ+ and decrease when the electron correlation method is changed from MP2 to CCSD(T). For the electrostatic complexes, the effect is mild, amounting to shifts of 1−2 kcal/mol. For the B^+ inserted products and the intervening transition state ($TS2_n$) the effect is larger, with relative binding energy shifts of 5−18 kcal/mol being observed. Finally, for the transition state between the electrostatic complexes and the covalent inserted products ($TS1_n$), the magnitude of the effect is intermediate, amounting to shifts of about 1−5 kcal/mol. These trends have been observed and discussed in previous studies[2,6] of sigma bond activation by cooperative interaction with B^+. In those studies, comparison to available experimental results and multireference configuration interaction calculations indicated that the CCSD(T) results with the pVTZ+ basis set were more accurate. Thus, those results will be emphasized in the current work.

$B^+/CH_4/H_2$. Geometric and energetic parameters characterizing stationary points on this hypersurface are summarized in Table 1 and illustrated in Figure 1. Although the electrostatic complex has C_1 symmetry, the local $B^+(CH_4)$ and $B^+(H_2)$ geometries are near C_{3v} and C_{2v}, respectively, as was observed previously[2,6] for these isolated complexes. The value of r(BC) is only about 0.03 Å longer than the value calculated[6] for $B^+(CH_4)$; however R is almost 0.4 Å longer than the value calculated[2] for $B^+(H_2)$. Inclusion of harmonic ZPE predicts that D_0 is 0.59 kcal/mol less than the D_e value of 18.63 kcal/mol.

Two B^+ inserted covalent structures are possible for this system: a CH inserted $CH_3BH^+(H_2)$ structure and an HH inserted $H_2CH_2BH_2^+$ structure, with HH insertion being more stable by about 4.0 kcal/mol. The electronic binding energy of H_2 with CH_3BH^+ in the CH inserted structure is about 5.4 kcal/mol and induces nearly a 35° bend in θ(HBC) from the linear equilibrium value of isolated CH_3BH^+. The HH inserted structure is structurally similar to diborane, with which it is isoelectronic, and the bonding in this structure, with special emphasis on the unusual CHB bridge bonds, has been discussed in detail elsewhere.[16] The transition state connecting these two structures ($TS2_1$) has C_s symmetry with $r(H_2)$ significantly elongated to 1.144 Å and both hydrogen atoms interacting strongly with boron at a distance of about 1.25 Å. From this

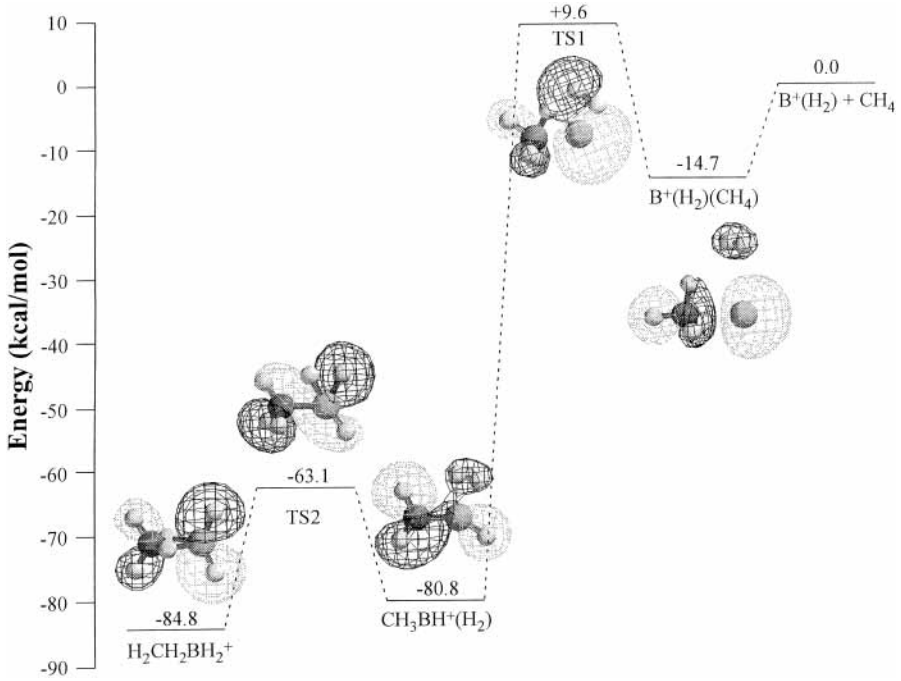

Figure 1. Relative energy of stationary points along the minimum energy reaction path for $B^+(H_2) + CH_4 \rightarrow B^+$ inserted products calculated at the CCSD(T)/pvTZ+//MP2/pVTZ+ level of theory with MP2/pVTZ+ harmonic ZPE added. The orbitals pictured show the evolution of the HOMO along the reaction path. In each structure, hydrogen atoms are represented by the small spheres, carbon by the dark sphere on the left side of the structure, and boron by the gray sphere on the right side of the structure.

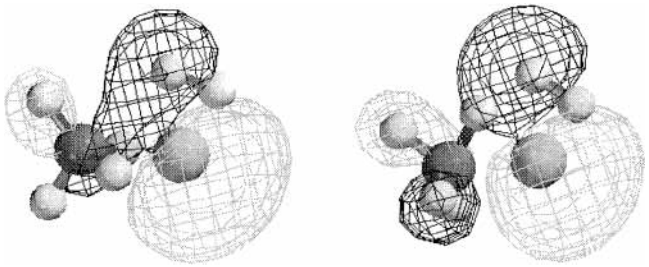

Figure 2. Comparison of the structure and HOMO of $TS1_1$ calculated at the MP2/pvDZ+ (left) and MP2/pVTZ+ (right) level of theory. In each structure, hydrogen atoms are represented by the small spheres, carbon by the dark sphere on the left side of the structure, and boron by the gray sphere on the right side of the structure.

geometry a decrease in $r(H_2)$ leads to the CH inserted structure, whereas an increase in $r(H_2)$ leads to a transfer of a hydrogen atom from boron to carbon forming the HH inserted structure. Remarkably, this sigma bond rearrangement pathway is fairly facile, with the transition state energy lying less than 20 kcal/mol above the energy of either structure.

The main transition state ($TS1_1$) for this system separates the electrostatic structure from the inserted covalent structures and lies only about 6.2 kcal/mol above the energy of $B^+ + CH_4 + H_2$ with ZPE included. In the MP2/pVTZ+ $TS1_1$ structure (Figure 1), $r(H_2)$ is significantly lengthened by almost 0.2 Å to 0.9193 Å, and the CH bond nearest the H_2 molecule is moderately lengthened by about 0.1 Å to 1.208 Å. As the system proceeds toward the CH inserted product, the hydrogen of this CH bond and one of the H_2 atoms combine to form a new H_2 molecule, while boron forms a bond with carbon and the other H_2 atom. Thus, the CH insertion product is formed without an actual B^+ insertion. Interestingly, $TS1_1$ calculated at the MP2/pVDZ+ level of theory is qualitatively different, as illustrated in Figure 2. With the pVDZ+ basis set, the methane molecule is rotated relative to the pVTZ+ $TS1_1$ so that two CH bonds interact with B^+, and no methane hydrogen is particularly close to the H_2 molecule. As the pVDZ+ $TS1_1$ structure proceeds toward insertion products, the HH insertion product is formed by the direct insertion of B^+ into the H_2 bond. Despite the structural and reaction path differences, the pVDZ+ $TS1_1$ is also calculated to have a relatively low energy, lying only about 9.5 kcal/mol above the energy of $B^+ + CH_4 + H_2$ with ZPE included. At both the pVDZ+ and pVTZ+ level of calculation, a search for the "other" type of transition state (i.e., a pVDZ+ type $TS1_1$ with the pVTZ+ basis set and vice versa) was conducted without success. In contrast to $TS1_1$, the structure of $TS2_1$ showed little basis set dependence.

$B^+/CH_4/2H_2$. Geometric and energetic parameters characterizing stationary points on this hypersurface are summarized in Table 2 and illustrated in Figure 3. The electrostatic structure again has C_1 symmetry with local $B^+(CH_4)$ and $B^+(H_2)$ geometries near C_{3v} and C_{2v}, respectively. Corresponding geometric parameters are very similar to those calculated for the $B^+(CH_4)(H_2)$ complex. At the pVTZ+ level, the two H_2 molecules are oriented in a near *T*-shaped structure, whereas at the lower pVDZ+ level, the two H_2 molecules are oriented parallel to each other, giving the complex an overall C_s symmetry. Inclusion of harmonic ZPE predicts that D_0 is 2.46 kcal/mol less than the D_e value of 20.83 kcal/mol.

As before, two B^+ inserted covalent structures are possible: a CH inserted $CH_3BH^+(H_2)_2$ structure and an HH inserted $BH_2^+(CH_4)(H_2)$ structure, with the HH inserted structure now being only 1.2 kcal/mol more stable than the CH inserted structure. In the HH inserted structure, a $BH_2^+(H_2)$ interaction forms at the expense of one of the CHB bridge bond interactions of the $n = 1$ structure, and in the equilibrium geometry, methane interacts with BH_2^+ through a single CHB bridge bond. In the CH inserted structure, the second H_2 molecule interacts with CH_3BH^+ in a manner very similar to that observed for $CH_3BH^+(H_2)$. In the intervening transition state ($TS2_2$) five hydrogen atoms interact strongly with boron: two forming a BH_2^+ like moiety, two at a near H_2 separation forming a $BH_2^+(H_2)$ interaction, and one interacting with carbon in a CHB bridge

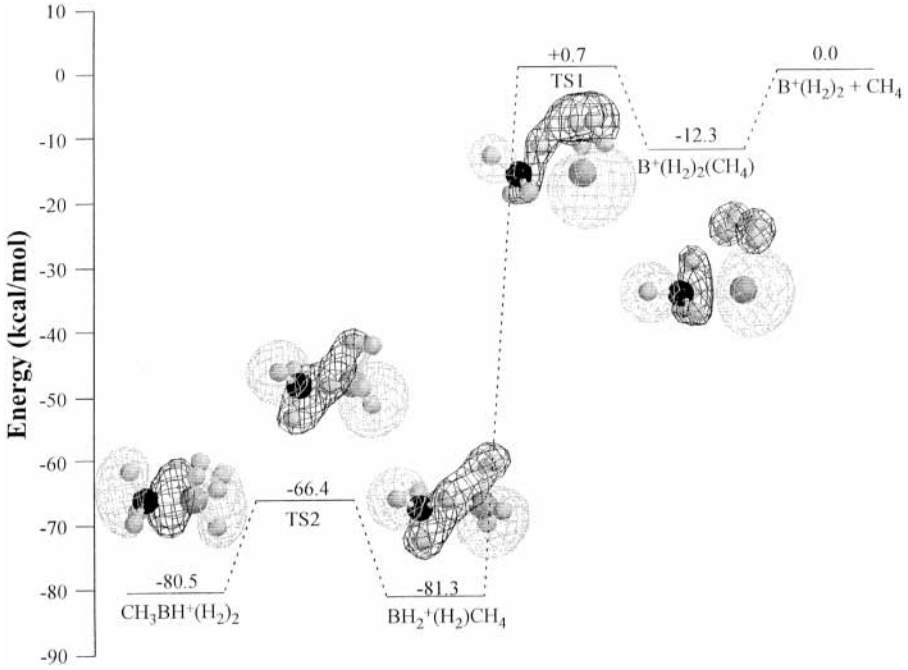

Figure 3. Relative energy of stationary points along the minimum energy reaction path for $B^+(H_2)_2 + CH_4 \rightarrow B^+$ inserted products calculated at the CCSD(T)/pvTZ+//MP2/pVTZ+ level of theory with MP2/pVTZ+ harmonic ZPE added. The orbitals pictured show the evolution of the HOMO along the reaction path. In each structure, hydrogen atoms are represented by the small spheres, carbon by the dark sphere on the left side of the structure, and boron by the gray sphere on the right side of the structure.

TABLE 2: Calculated Geometries and Relative Energies for $B^+/CH_4/2H_2$ Stationary Points

property	electrostaric complex	transition state 1	$BH_2^+CH_4(H_2)$	transition state 2	$CH_3BH^+(H_2)_2$
point group	C_1	C_s	C_s	C_s	C_s
$r(H_2)$/Å	0.7435, 0.7427	0.7989, 0.7989	0.8138, 0.8138	0.7715, 0.8041	0.8007, 0.8007
R/Å	2.5711, 2.6924	1.6788, 1.6788	1.3482, 1.3482	1.5237, 1.3784	1.3735, 1.3735
r(BC)	2.0626	2.1018	2.0611	1.5522	1.5676
R(BH)			1.1762	1.1805	1.1856
$\theta(R,r(H_2)$/deg	99.5, 91.4	112.9, 112.9	90.0, 90.0	94.5, 89.8	89.9, 89.9
$\theta(R,r$(BC)/deg	90.1, 93.4	98.3, 98.3	115.9, 115.9	113.2, 116.9	112.1, 112.1
θ(BCH′)/deg	173.0	147.3			
$\theta(R,R')$/deg	75.6	81.2			98.8, 98.8
θ(HBC)/deg				131.2	127.5
relative energy					
MP2/pVDZ+	−20.86	−12.34	−103.68	−90.03	−92.38
CCSD(T)/pVDZ+	−19.65	−8.48	−93.21	−77.75	−80.22
MP2/pVTZ+	−22.09	−14.35	−108.32	−95.27	−109.68
CCSD(T)/pVTZ+	−20.83	−11.41	−99.42	−84.42	−98.94
relative ZPE	2.46	6.06	13.41	11.96	14.24

bond. If the system moves from $TS2_2$ toward the CH inserted structure, the bridging hydrogen and one of the BH_2^+ hydrogen atoms combine to form the second H_2 molecule. Alternatively, if the system moves from $TS2_2$ toward the HH inserted structure, all five hydrogen atoms maintain their interactions with most of the motion involving an increase in the BH_2^+ bond angle. This sigma bond rearrangement pathway is even more facile than the $n = 1$ path, with $TS2_2$ lying only about 15 kcal/mol above either B^+ inserted product.

Calculations with either the pVDZ+ or pVTZ+ basis sets gave qualitatively similar structures for the main transition state ($TS1_2$) of the $n = 2$ system which separates the electrostatic structure from the inserted covalent structures and lies about 5.3 kcal/mol *below* the energy of $B^+ + CH_4 + 2H_2$ with ZPE included. In contrast to $TS1_1$, $r(H_2)$ in $TS1_2$ is only mildly elongated from the isolated equilibrium value, with the major geometric change from the electrostatic complex being about a 0.9 Å decrease in R. As the system proceeds toward the HH inserted product, one hydrogen atom from each of the hydrogen molecules forms a bond with B^+, while the other hydrogen atoms from each hydrogen molecule bond to each other to form a new H_2 molecule.

Discussion

It is convenient to consider the results grouped by bonding arrangements under the headings of electrostatic complexes, B^+ inserted products, and the main intervening transition state ($TS1_n$) between these structures. The transition states connecting the CH and HH inserted products ($TS2_n$) will be grouped with those products.

Electrostatic Complex. The near T-shaped orientations of the H_2 molecules with respect to B^+ ($\theta(R,r(H_2) \approx 90°$), and H_2 with respect to H_2 in the $n = 2$ complex, have been observed previously[2] and can be understood in terms of an ion−quadrupole interaction and an quadrupole−quadrupole interaction, respectively. The "face-on" orientation of methane with respect to B^+ (θ(BCH′) $\approx 180°$) has similarly been observed previously[6] and explained in terms of minimizing B^+/CH_4 short-range repulsion. Using previously calculated[2,6] D_e values for $B^+(H_2)$, $B^+(H_2)_2$, and $B^+(CH_4)$ (4.3, 8.4, and 16.5 kcal/mol with

respect to $B^+ + nH_2$ or CH_4, respectively) and the present D_e values for $B^+(CH_4)(H_2)_n$, the mixed electrostatic cluster binding energy is found to be 2.2 and 4.1 kcal/mol less than the sum of the constituent binding energies for $n = 1$ and 2, respectively. An interpretation of this result in terms of an approximate halving of the $B^+(H_2)$ binding energy resulting from the simultaneous interaction of B^+ with CH_4 is supported by the following four considerations. (1) The sequential $B^+(H_2)_n$ binding energy changes by less than 5% for $n < 4$, indicating relatively independent electrostatic binding with respect to H_2. (2) Sequential $B^+(CH_4)_n$ binding energy decreases by up to 50% for $n < 4$, indicating strong nonindependent binding with respect to CH_4. (3) The value of r(BC) in the mixed complexes is only about 0.04 Å longer (2% change) than the value in $B^+(CH_4)$, indicating that the H_2 binding has little effect on CH_4 binding. However, (4) the value of R in the mixed complexes is approximately 0.36 Å longer (16% change) than the value in $B^+(H_2)_n$, indicating that CH_4 binding significantly weakens H_2 binding in the mixed complexes.

B^+ Inserted Products. The calculated structures of the CH inserted products, $CH_3BH^+(H_2)_n$, are exactly what would be anticipated from a consideration of the structures of $BH_2^+(H_2)_n$ and viewing CH_3BH^+ as a methyl-substituted BH_2^+ ion.[2,17,18] In particular, the one or two H_2 molecules form 3c−2e bonds with boron, formally completing its octet with $n = 2$. However, while the sequential electronic binding energies of H_2 with BH_2^+ are 18.9 and 22.8 kcal/mol for $n = 1$ and 2, respectively, the corresponding sequential electronic binding energies with CH_3BH^+ are substantially smaller, being only 5.4 and 9.4 kcal/mol. It is interesting to note that in both cases the second sequential binding energies are larger than the first. This is unusual for a simple electrostatic interaction, but consistent with the increased electronic stability associated with completing the boron electronic octet. The decreased H_2 binding energy resulting from the methyl substitution can be understood from a consideration of the electron-donating capability of methyl and by viewing BH_2^+ as a Lewis acid, as has been analyzed in detail elsewhere.[16] When ZPE effects are considered, the predicted sequential binding energy of H_2 to CH_3BH^+ falls to only 0.62 and 0.53 kcal/mol for $n = 1$ and 2, respectively, suggesting that these ions may be difficult to observe.

The bonding and structure of the diborane-like $n = 1$ HH inserted product have been analyzed in detail previously.[16] That work showed that the extraordinarily strong CH_4/BH_2^+ interaction ($D_e = 35.5$ kcal/mol) arises from two unusual CHB, 3c−2e bridge bonds that serve to complete the boron electronic octet. In the $n = 2$ case, an interesting competition between 3c−2e bonding involving CH or HH with the BH_2^+ moiety is won by H_2. Although this H_2 molecule is bound by a covalent 3c−2e bond with boron, the binding energy is uncharacteristically weak (3.3 kcal/mol) because a CHB 3c−2e bond is readily formed upon the removal of the H_2. Taking the electrostatic binding energy of H_2 with $BH_2^+(H_2)_2$ (2.2 kcal/mol)[2] as a measure of the interaction energy of H_2 with a completed octet BH_2^+, the mixed 3c−2e bonding (CH and HH) can be estimated to be about 1 kcal/mol more stable than a structure with two CHB bridge bonds and an electrostatic interaction with H_2. However, such a structure appears to be hypothetical because a corresponding local energy minimum could not be located.

For the $n = 1$ case, the two inserted products and the intervening transition state ($TS1_1$) have been studied previously[17] in context of the $BH_2^+ + CH_4$ reaction, and the present results agree well with that work. For both $n = 1$ and 2, $TS2_{1,2}$ allows the conversion of a CH and a BH bond in the HH inserted product to a CB bond and an HH bond in the CH inserted product and vice versa. Perhaps the most remarkable aspect of this chemical transformation is that it takes place with an activation energy of less than 20 kcal/mol. Considering the mechanism, it is likely that an analogous reaction would proceed for any saturated hydrocarbon. Indeed, it is possible that the reaction would proceed with CH bonded to a variety of atoms and functional groups, although possible competing reactions would need to be considered.

Transition State 1. The remarkably low energy of the transition states ($TS1_n$) separating the reactants $B^+(H_2)_n + CH_4$ and the boron insertion products can be understood in terms of the node evolution of the highest occupied molecular orbital (HOMO) shown in Figures 1−3. Focusing first on the pVTZ+ results, the node positioned between B^+ and the electrostatically bound CH_4 and nH_2 molecules is maneuvered to intersect HH and CH bonds or two HH bonds as the system moves toward $TS1_1$ or $TS1_2$, respectively. As the system moves toward a boron inserted product, the two bonds intersected by the node in the HOMO (HH and CH or two HH) break, a new HH bond is formed, and a new BC ($n = 1$) or BH ($n = 2$) bond is formed in a concerted pericyclic mechanism. This is the same mechanism identified in the $B^+ + 2H_2 \rightarrow BH_2^+ + H_2$ reaction,[2] which had a calculated activation energy, including ZPE effects, of 11.6 kcal/mol with respect $B^+(H_2) + H_2$. Thus, considering the comparable strength of CH and HH bonds, the 9.6 kcal/mol activation energy of the $n = 1$ system mimics the all-hydrogen system and further illustrates the generality of this cooperative sigma bond activation mechanism even when different types of sigma bonds are involved.

For the $n = 2$ case, $TS1_2$ is identical to the corresponding transition state in the $B^+ + 2H_2 \rightarrow BH_2^+ + H_2$ reaction. Thus, the dramatic decrease in activation energy to near zero with the participation of CH_4 is best attributed to general solvent-like electrostatic interaction rather than some specific chemical participation. This conclusion is supported by the magnitude of the activation energy lowering (approximately 14.6 kcal/mol) that is comparable to the B^+/CH_4 electrostatic interaction energy (16.6 kcal/mol with ZPE considerations[6]). This interpretation suggests that a similar effect might occur with methane replaced by suitable molecules with a sufficiently large electrostatic interaction with B^+. Considering the facile rearrangement of CH, BH, HH, and CB bonds, which are possible following B^+ insertion, this or analogous chemistry may provide efficient routes for hydrogenation reactions as well as sigma bond activation. In principle, experimental studies of low-energy collisions of $B^+(H_2)_2$ with CH_4 (and other molecules) could be performed using mass spectrometric techniques similar to those used to study $B^+(H_2)_n$ formation and reactivity.[7] Such an experiment would directly test the interesting mechanistic prediction that a $B^+(H_2)(D_2)$ reactant would initially produce the mixed isotopic product, BHD^+, exclusively.

It remains to consider the variation in $TS1_1$ observed for the pVDZ+ and pVTZ+ basis sets (Figure 2). The pVTZ+ results have just been considered in detail and need no further elaboration. The pVDZ+ $TS1_1$ has three sigma bonds, two CH and one HH, simultaneously interacting with B^+, while the node in the HOMO orbital intersects only the HH bond. Previous studies[6] of $B^+ + nCH_4$ have shown that CH_4 can participate in the cooperative interaction mechanism as either a one or two sigma bond contributor. In pVDZ+ structures, CH_4 is operating as a two sigma bond contributor, and the reaction proceeds by direct insertion of B^+ into the HH bond rather than by the pericyclic mechanism occurring in the pVTZ+ case, where CH_4

contributes only one sigma bond. This result is completely analogous to the change from a pericyclic to a direct insertion mechanism observed[2] for $B^+(H_2)_n$ as *n* increased from 2 to 3 (i.e., the number of cooperating sigma bonds increased from 2 to 3). The change in the methane mechanistic participation with basis set size suggests that these two possibilities are energetically similar and may proceed in competition. If the gas phase reaction of $B^+ + CH_4 + H_2$ could be observed, the expected products would be BH_2^+ with eliminated CH_4 carrying away the energy, or CH_3BH^+ with eliminated H_2 carrying away the energy, from the pVDZ+ or the pVTZ+ transition state, respectively.

Acknowledgment. We gratefully acknowledge the Robert A. Welch Foundation and the Petroleum Research Fund administered by the American Chemical Society, under Grant No. 33631-AC6, for partial support of this work.

References and Notes

(1) Arndtsen, B. A.; Gergman, R. G.; Mobley, T. A.; Peterson, T. H. *Acc. Chem. Res.* **1995**, *28*, 154.

(2) Sharp, S. B.; Gellene, G. I. *J. Am. Chem. Soc.* **1998**, *120*, 7585−7593.

(3) Sharp, S. B.; Lemoine, B.; Gellene, G. I. *J. Phys. Chem. A* **1999**, *103*, 8309−8316.

(4) Sharp, S. B.; Gellene, G. I. *J. Chem. Phys.* **2000**, *113*, 6122−6131.

(5) Sharp, S. B.; Gellene, G. I. *J. Phys. Chem. A* **2000**, *104*, 10951−10957.

(6) Bell, C. J.; Gellene, G. I. *Faraday Discuss.* **2001**, *118*, 477−485.

(7) Kemper, P. R.; Bushnell, J. E.; Weis, P.; Bowers, M. T. *J. Am. Chem. Soc.* **1998**, *120*, 7577.

(8) Nichols, J.; Gutowski, M.; Cole, S. J.; Simons, J. *J. Phys. Chem.* **1992**, *96*, 644.

(9) Ruatta, S. A.; Hanley, L.; Anderson, S. L. *J. Chem. Phys.* **1989**, *91*, 226.

(10) Armentrout, P. B. *Int. Rev. Phys. Chem.* **1990**, *9*, 115.

(11) Lin, K. C.; Watkins, H. P.; Cotter, R. J.; Koski, W. S. *J. Chem. Phys.* **1974**, *60*, 5134.

(12) Dunning, T. H., Jr. *J. Chem. Phys.* **1989**, *90*, 1007.

(13) Kendall, R. A.; Dunning, T. H., Jr.; Harrison, R. J. *J. Chem. Phys.* **1992**, *96*, 6796.

(14) Raghavachari, K.; Trucks, G. W.; Pople, J. A.; Head-Gordon, M. *Chem. Phys. Lett.* **1989**, *157*, 479.

(15) Frisch, M. J.; Trucks, G. W.; Schlegel, H. B.; Gill, P. M. W.; Johnson, B. G.; Robb, M. A.; Cheeseman, J. R.; Keith, T.; Petersson, G. A.; Montgomery, J. A.; Raghavachari, K.; Al-Laham, M. A.; Zakrzewski, V. G.; Ortiz, J. V.; Forseman, J. B.; Peng, C. Y.; Ayala, P. Y.; Chen, W.; Wong, M. W.; Andres, J. L.; Replogle, E. S.; Gomperts, R.; Martin, R. L.; Fox, D. J.; Binkley, J. S.; Defrees, D. J.; Baker, J.; Stewart, J. P.; Head-Gordon, M.; Gonzalez, C.; Pople, J. A. *Gaussian 94*, revision B.3; Gaussian, Inc.: Pittsburgh, PA, 1995.

(16) McDonald, L. E.; Gellene, G. I. *Mol. Phys.* **2001**, *99*, 377.

(17) DePuy, C. H.; Gareyev, R.; Hankin, J.; Davico, G. E.; Damrauer, R. *J. Am. Chem. Soc.* **1997**, *119*, 427.

(18) DePuy, C. H.; Gareyev, R.; Hankin, J.; Davico, G. E.; Krempp, M.; Damrauer, R. *J. Am. Chem. Soc.* **1998**, *120*, 5086.